

## Synthesis and applications of metal nanoparticles (Au, Ag)@C-graphene oxide and carbon nanotubes hybrid nanoarchitectures

P. Kavitha<sup>a,\*</sup>, C. Shanthi<sup>a</sup>, R. Kannan<sup>b</sup>

<sup>a</sup>*Department of Physics, Sona College of Technology (Autonomous), Salem - 636 005, Tamil Nadu, India*

<sup>b</sup>*Department of Chemistry, Sri Kumara Gurupara Swamigal Arts College, Srivaikuntam, Affiliated to Manonmaniam Sundaranar University, Tirunelveli. Tamilnadu, India*

In this work, we made an effort to use dopamine hydrochloride and the solid state method to anchor the gold and silver metallic nanoparticles over the graphene oxide-carbon nanotubes to improve the metal nanoparticles' interaction with the support materials. Because the hybrid nanoarchitectures of graphene-CNT provide enhanced electron transfer ability, which facilitates the catalytic activity more quickly and enhances the rate. Additionally, carbon nanotubes-graphene oxide-metal nanoparticles based hybrid catalyst was developed in a similar fashion. The formation of metallic nanoparticles in a size range of 3–15 nm is visible in the micrographs. These particles developed as nano-islands. The excess reductant formed as polydopamine acts as a stabilizer, and further, we utilise this polydopamine into carbon by the calcination process. It results that carbonous materials will enhance the interaction between metal and support (CNT/GO). This leads to improved catalytic activity towards the reduction of 4-nitrophenol and catalytic decolorization of methylene blue at room temperature. The suggested technique for synthesizing metal nanoparticles over carbon nanostructures is simple and environmentally friendly.

(Received February 29, 2024; Accepted June 7, 2024)

*Keywords:* Graphene oxide, Metallic nanoparticles, Hybrid catalyst, Carbon nano structures, Polydopamine, 4-nitrophenol, Methylene blue, Catalytic decolourization

### 1. Introduction

The graphene-based nanostructures could have promising applications in many fields due to their strong and stable nature, chemical and thermal stability. Conversely, metal nanostructures are gaining a lot of interest because of their potential uses in energy storage, conversion, sensors, and catalysis [1-6]. Metal nanostructures have been used as catalysts extensively in recent times, particularly noble metals like palladium (Pd), platinum (Pt), silver (Ag), and gold (Au) [7, 8]. The development of these MNPs has been achieved by different methods based on the specific applications. Along with this, controlling the size and shape is a vital phenomenon because it tailors the activity towards applications. Assembling the metal nanostructures with graphene microscale nanosheets for practical applications is a great challenge.

One strategy to increase active site exposure is the 3D structuring of carbon materials. Graphene has high electronic conductivity. It does, however, tend to restack, resulting in a lower catalytic utilization. To prevent its restacking, several approaches have been reported, and one among them is to form a hybrid with carbon nano tubes, which functions as a spacer for graphene nanosheets. Additionally, it provides excellent electrical conductivity and catalytic activity due to its tunneling efficiency [9].

The paper, leather, and textile industries discharge massive quantities of dye-containing coloured wastewater into water resources. The majority of these dyes have harmful effects on both human health and the environment. The discharges also contain other extremely hazardous

---

\* Corresponding author: kavithap@sonatech.ac.in  
<https://doi.org/10.15251/DJNB.2024.192.845>

chemical compounds, which cause environmental problems [10, 11]. However, these dyes in water bodies reduce sunlight penetration, raise the oxygen demand for chemical and biological processes (BOD and COD), prevent photosynthesis, and restrict plant growth [12, 13]. Varieties of treatments, including chemical, physical, biological, and hybrid approaches, are employed to remove colour. Among them, chemical oxidation with an appropriate catalyst attracts attention because it is a quick and simple process that degrades the dyes [14, 15].

Nitro aromatics are important class of compounds used in the production of explosives, pesticides, herbicides, colorants, etc. Among them, 4-Nitrophenol (4-NP) is employed in the preparation of a number of artificial dyes. Additionally, 4-NP is a bio-refractory pollutant that is toxic and causes significant harm to the environment and the affect the internal organs of animals and human beings. Thus, 4-NP and its derivative products are common pollutants in many natural waters and industrial wastewater. Thus, we made an attempt to synthesize graphene oxide-CNT@C-MNPs (M=Au, Ag, AuAg) nano hybrids by in situ process to study the catalytic reduction of 4-NP. Room-temperature Au, Ag, and Au-Ag NPs with sizes ranging from 3 to 10 nm are produced by the above described method. Detailed studies for this research work are given.

## 2. Experimental

Figure 1 depicts the reaction scheme for the synthesis of metal nanoparticles Au, Ag@C-graphene oxide and carbon nanotubes hybrid nano architectures.

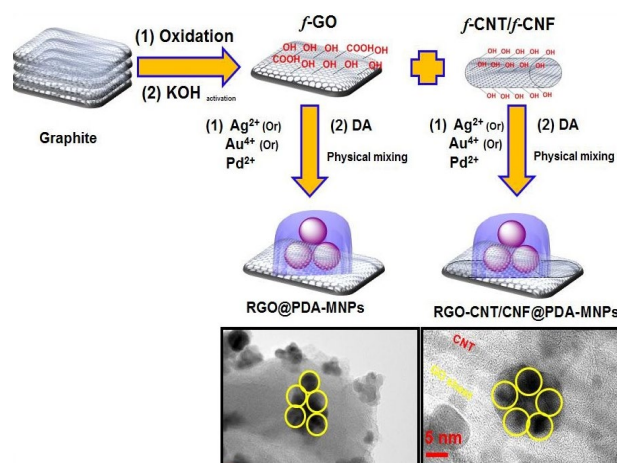


Fig. 1. Scheme of synthesis of metal nanoparticles AuAg@C-RGO-CNT-PDA nanoarchitectures.

## 3. Materials

We have received multiwall carbon nanotubes from Samsun Chemicals, located in the Republic of Korea. We have received Ascorbic acid (AA) and graphite powder from Alfa Aesar Chemicals, located in the Republic of Korea. We have acquired silver nitrate, chloroauric acid, and dopamine hydrochloride from Sigma-Aldrich. Ranchem (India) supplied hydrogen peroxide, hydrochloric acid, and potassium permanganate. Without additional purification, analytical-quality chemical substances have been purchased and utilized as received.

### 3.1. Synthesis of graphene oxide (GO)

GO was synthesized by chemically oxidizing graphite powder using the Hummer method [16, 17]. To put it briefly, 5.0 g of natural graphite powder and 80 ml of concentrated sulfuric acid were combined and stirred in an ice bath at a temperature between 0 to 2 degrees Celsius. Subsequently, 14.0 g of potassium permanganate was added gradually while stirring vigorously to maintain the suspension's temperature below 20°C. The reaction system was stirred for about an

hour and kept in an oil bath at 45°C after 15 minutes. Following that, 150 mL of water was then included and the mixture was stirred for 30 minutes at 90 °C.

After adding 500 mL more water to this, 40 mL of 30% hydrogen peroxide were added gradually. To remove the manganese ions from the filtrate, this mixture was filtered and then rinsed using a 1:10 aqueous solution of hydrochloric acid (250 mL). Using ultrasonic irradiation, the resultant solid was dried in the air and diluted to make an aqueous dispersion of graphite oxide.

The Multi walled carbon Nanotubes were mixed with solid KOH using mortar. After few minutes of grinding, a black paste like material formed and it was dispersed in DD water and washed several time to remove unreacted KOH. After that the *f*-CNT was dispersed in DD water for further use.

### 3.2. Synthesis of AuAg@C-RGO-CNT-PDA nanohybrid catalyst

The Au, Ag, and AuAg-MNPs on graphene oxide/CNT hybrid were developed by two processes, namely using ascorbic acid and dopamine as reducing agents.

Approximately 5 mg of  $\text{H}_4\text{AuCl}_6$  and 5 mg of  $\text{AgNO}_3$  and 15 mg of GO and 5 ml of functionalized multiwall carbon nanotubes was blended well with a mortar, then about 20 mg of solid ascorbic acid was added to the mixture and ground well. After that, the solid was then calcined at 800 °C and dried for around two hours at 90 °C in a hot air oven. Following this, 2 g of solid dopamine salt and RGO-CNT@C-AuAg were combined and thoroughly mixed using a mortar. The solid material was separated after five minutes, dried for two hours at 90° C in a hot air oven, and labeled as AuAg@C-RGO-CNT-PDA. Mono metals like Au and Ag on graphene oxide are made in a similar manner.

### 3.3. Characterization

The crystalline phases of the prepared catalysts are characterized by the powder X-ray diffraction method (XRD, Shimadzu Instrument diffractometer with  $\text{Cu K}\alpha$  radiation). The Fourier Raman spectra are studied using a Nanofinder 30 confocal Raman microscope (Tokyo Instrument Co., Japan, 500–3200  $\text{cm}^{-1}$  with a He–Ne laser beam of 633 nm wavelength). The Fourier Transform Infrared (FT-IR) spectra are recorded on a Perkin Elmer (Spectra GX) spectrometer in the 400–4000  $\text{cm}^{-1}$  range. With an  $\text{Al K}\alpha=1486.6$  eV excitation source, the elemental compositions of the as prepared catalysts are analyzed using X-ray Photoelectron Spectra (XPS) captured using an Axis-Nova (Kratos Inc.).

Additionally, for the elements present in the catalyst in quantity, the surface properties of the catalysts are examined using Scanning Electron Microscopy (SEM) equipped with an Energy Dispersive X-ray Spectrometer (EDS) on a JEOL JSM-6200 equipped with an Oxford instrument at an accelerating voltage of 5–20 kV. Using a JEOL 2100 electron microscope running at 200 kV, High Resolution Electron Microscopy (HRTEM) images were captured.

### 3.4. Catalytic studies

The AuAg@C-RGO-CNT-PDA nanocomposite exhibits catalytic activity by decolorizing Methylene blue dye. The following is the 4-NP reduction reaction: A quartz cuvette with a length of 4.5 mL was filled with approximately 1.6 mL of 4-nitrophenol (0.1 mmol L<sup>-1</sup>) and an ice-cold  $\text{NaBH}_4$  aqueous solution (0.10 mL of 0.10 mol L<sup>-1</sup>). The above solution was then given a gentle shake to dissolve 20 mg of metal catalyst. The optical absorption spectrum of 4-nitrophenol was measured at 100-second intervals between 200 and 500 nm to characterize the reduction reaction.

The batch technique of decolorizing Methylene blue (MB) dye was used for the catalytic investigations. A 100 mL conical flask was filled with approximately 100 mL of MB dye solution (Sigma-Aldrich, 0.01 mmol) and 20 mg of various catalysts (Au@CCNT/RGO, Ag@C-CNT/RGO, and AuAg@C-RGO-CNT-PDA) were added while continuously stirring. A slow addition of 1 mL of  $\text{H}_2\text{O}_2$  was made after 2 minutes. Room temperature was used to allow the mixture to react. After that, at various intervals, a portion of the solution was taken, split, centrifuged, and examined with a Wensar double beam UV-visible spectrophotometer.

## 4. Results and discussion

Several studies have shown that AA effectively reduces metal nanoparticles, particularly Ag and Au. Our earlier studies [18, 19] show the excess of AA, after reduction of metal into MNPs, will serve as a stabiliser and form nanofibers. In the earlier work, we have tried the same in the different carbon supports namely graphene oxide, carbon Nanotubes, carbon nanofibers [20-22]. It demonstrates excellent formation of nanoparticles into carbon nano architectures.

In this work, the development of active interaction between carbon nanotubes and graphene with metal nanoparticles with the help of polydopamine was explored. Compared to AA, the PDA shows excellent polymeric film which helps to bind the MNPs and CNTs on the graphene oxide platform.

### 4.1. X ray diffraction studies

As seen in Figures 2 and 3, the XRD analysis shows demonstrate the existence of Au and Ag MNPs over the CNT/graphene oxide hybrid. Initially, the phase change in multiwalled carbon nanotubes and graphene oxide hybrid using poly dopamine was analysed using XRD. The functionalized MWCNT shows characteristic peaks of 2q at 25.2 and 43. And RGO/CNT hybrid with PDA shows similar peaks at the same positions with a slight shift in the peak positions. Additionally, hybrid nanostructures show a small hump around 12-25, which is presumed to be a polymeric form of DA.

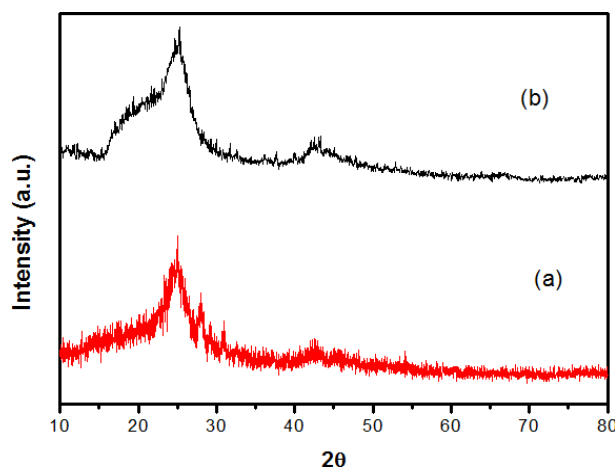


Fig. 2. XRD Spectrum of (a) f- CNT (b) CNT/RGO@PDA.

The AuAg (311), (220), (200), and (111) peaks are represented by the XRD peaks at 79.1, 65.2, 44.1, and 39.1, respectively. The originally identified Au NPs peak values were somewhat moved from these peaks. Reduced graphene oxide is present because the C(002) peak ( $2\theta=10.3$ ) is absent and a new broad peak appears between ( $2\theta$ ) 15 to 25. This indicates the metal and graphene oxide results are produced simultaneously in this process. The AuAg-AA/DHA-GO was subjected to thermal and microwave heating. Figure 3c and 3d correspond to microwave and thermal heating, and both the methods show almost similar crystalline patterns. However, the complete carbonization was achieved on thermal annealing.

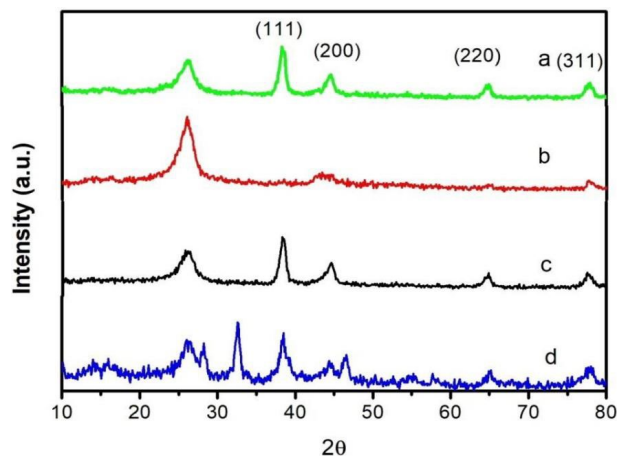


Fig. 3. XRD Spectrum of (a) RGO@AuAg, (b) CNT@AuAg, (c) CNT-RGO@AuAg, (d) AuAg@C-RGO-CNT-PDA.

#### 4.2. Scanning electron microscope and EDS studies

The topological characteristics were analyzed by SEM and HRTEM techniques. The EDX profile (Figure 4d) verifies the existence of Ag and Au over the catalyst, and the SEM images (Figure 4 a-c) demonstrate a uniform distribution of MNPs (AgAu) on the MWCNTs-RGO PDA nanohybrids.

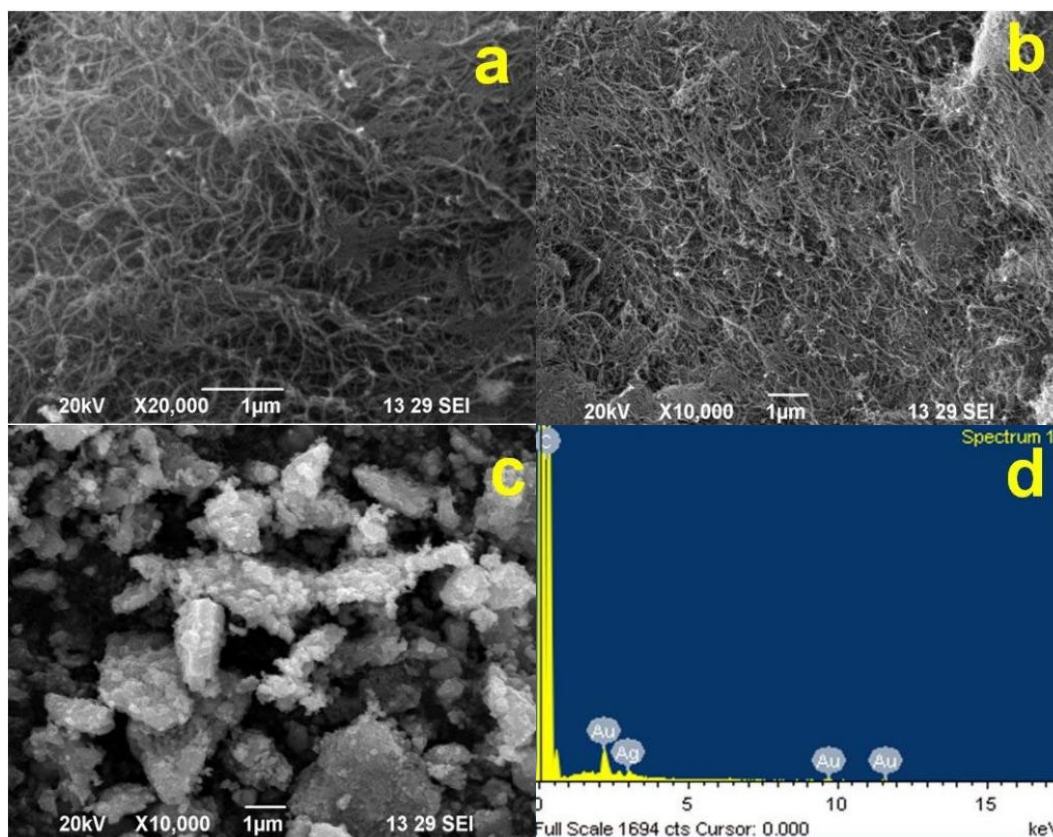
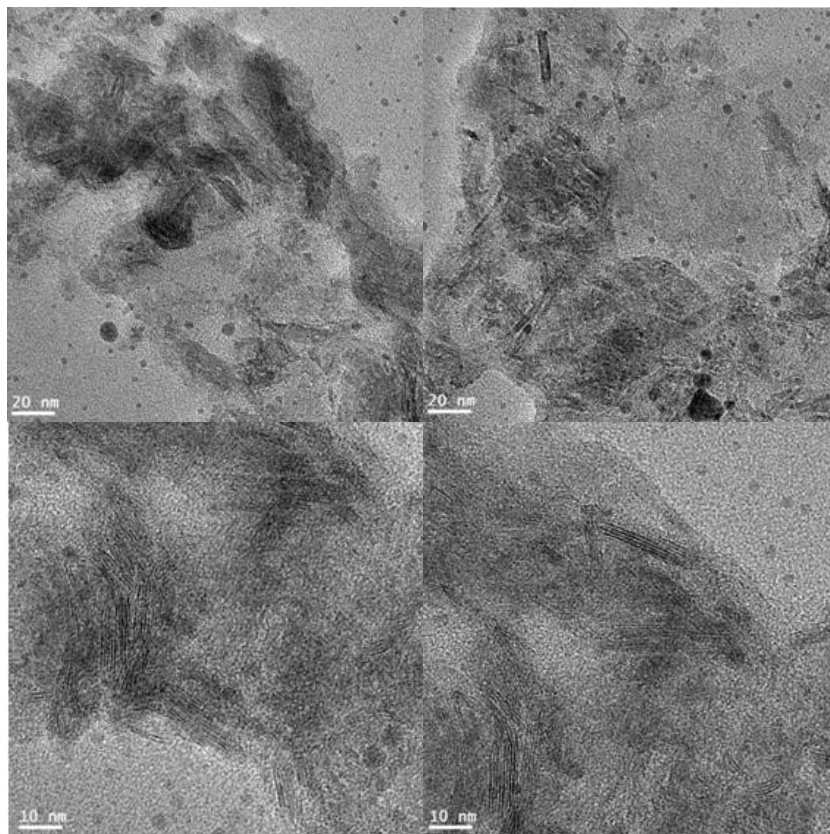


Fig. 4. SEM images and EDS profile of the synthesized AuAg@C-RGO-CNT-PDA catalyst.

### 4.3. Transmission electron microscope studies

Graphene sheets, AuAg, and MWCNT compressed into polymeric nanoarchitectures of dopamine are easily seen when examined with higher magnification HRTEM. The micrographs show that metal nanoparticles, like AuAg, originated as uniformly distributed, tiny particles with a size range of 2 to 10 nm. Furthermore, the graphene oxide nanosheets edges and the spaces between them developed metal nanoparticles, as depicted in Figure 5.



*Fig. 5. TEM images of the synthesized AuAg@C-RGO-CNT-PDA catalyst.*

### 4.4. X Ray photoelectron spectral studies

An analysis is conducted on the prepared AuAg@C-RGO-CNT-PDA state, and the XPS spectrometer is shown in Fig. 6. The binding energy of C1s is indicated by the peak at 284.3 eV. Moreover, Au 4f<sub>7/2</sub> and 4f<sub>5/2</sub> have binding energies of 83.9 and 87.6 eV, respectively, which match the NPs made of gold. Additionally, silver NPs are indicated by Ag 3d<sub>3/2</sub> and Ag 3d<sub>5/2</sub> at 374.1 and 385.2 eV, respectively. [23, 24]. The above experimental spectrum clearly indicates the formation of AuAg@C-RGO-PDA.

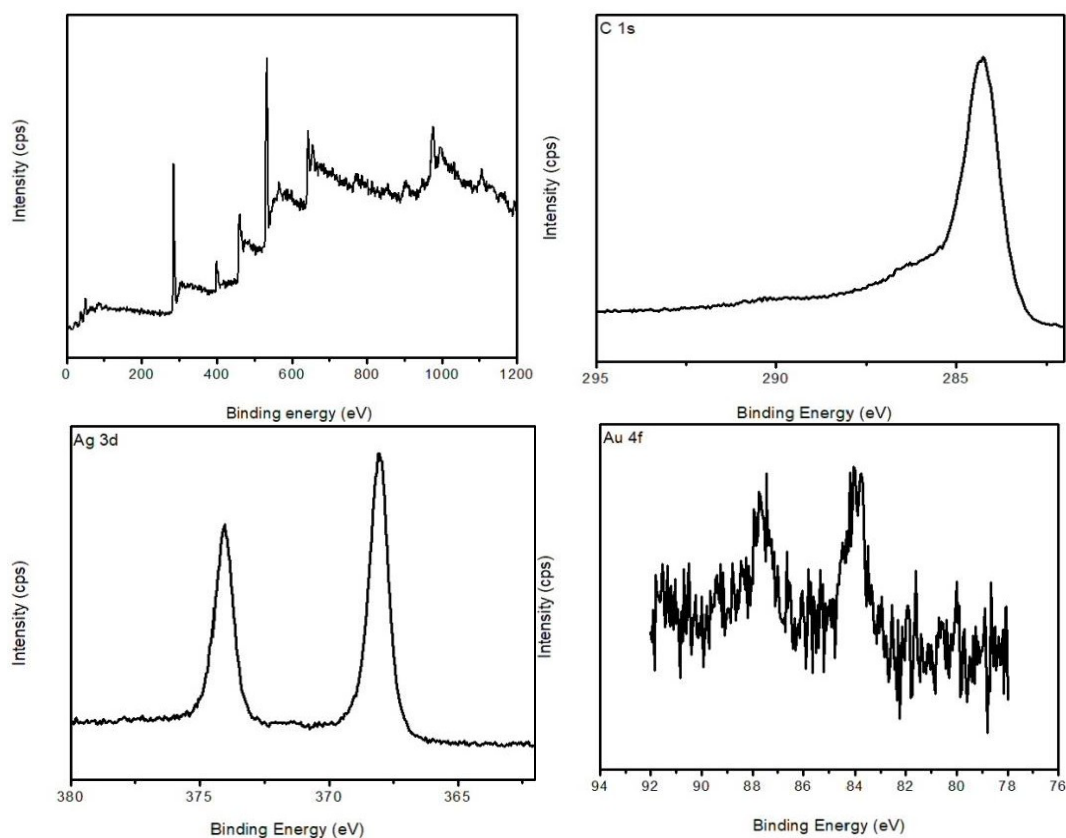


Fig. 6. XPS profile of AuAg@C-RGO-CNT-PDA.

#### 4.5. Catalytic studies

The oxidative degradation of Methylene blue dye and the reduction of 4-nitrophenol have been used to test AuAg@C-RGO-CNT-PDA's catalytic activity. Figure 7 shows the initial oxidation of Methylene blue dye in the presence of RGO-CNT, AuAg@C-RGO-CNT-PDA, and sodium borohydride ( $\text{NaBH}_4$   $0.5 \times 10^{-5}$  M). The UV spectrum revealed a negligible decrease in absorbance when MNPs were not present. However, the CNT/RGO@PDA- AuAg catalyst showed excellent catalytic degradation of 98% in 75 min. However, the catalytic surface will be highly affected by the  $\text{NaBH}_4$ .

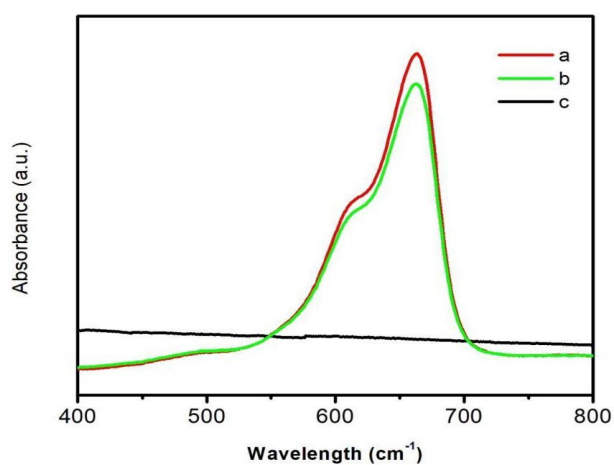


Fig. 7. UV-Vis. Spectrum of (a) MB dye, catalytic degradation of MB with (b) Graphene/CNT and (c) AuAg@C-RGO-CNT-PDA hybrid catalyst with  $\text{H}_2\text{O}_2$ .

Thus further recovery and reuse is highly difficult. Hence for the further studies, we have proceeded with the dye degradation. Additionally, it is observed that the UV spectrum (Figure 7) showed a straight line, which implies that the decolorization followed by the mineralization of dye molecules occurred during the course of the reaction. These results clearly show the degradation of organic pollutants under the experimental conditions. To evaluate further the dye concentration, catalyst quantity, reaction time, and recyclability, batch studies were conducted.

The concentration of dye solution at low concentration the degradation was very high (0.1 mg/L) i.e. about 95%, where at higher concentration (2.0mg/L) it is reduced up to 28% for Au-Ag-CNT@C-graphene and expressed in Figure 7 (UV-Vis.). From the UV-Vis. spectral studies, it is clear that the metal MNPs such as AgAu, which act as excellent catalysts towards dye degradation. Hence, for further studies, we have compared the catalytic degradation profile of MB with AuAg@C, AuAg@C- Graphene/CNT, and AuAg@C-RGO-CNT-PDA hybrid catalyst with H<sub>2</sub>O<sub>2</sub>.

The results showed that both AuAg@C-Graphene/CNT and AuAg@C-RGO-CNT-PDA exhibit almost similar catalyst responses. However, AuAg@C-Graphene/CNT showed superior performance over CNT/RGO@PDA-AuAg. It was accounted as in the AuAg@C- Graphene/CNT, the reductants such as AA or DHA were converted as carbogenous products. It will provide a better platform for the catalyst, resulting in better interaction between MNPs and dye, which in results higher catalytic activity.

PDA serves as a good reducing agent and support for the AuAg@C-RGO-CNT-PDA, which will improve the catalyst and support's ability to transfer electrons. In the low concentration of MB dye (0.1mg/L), the degradation's effect at AuAg@C-Graphene/CNT is superior than AuAg@C-RGO-CNT-PDA hybrid catalyst, whereas at higher concentration (2.0 mg/L) the degradation was reversed, the AuAg@C-RGO-CNT-PDA hybrid catalyst showed higher degradation over other one. This may be due to the uniform distribution of MNPs and effective adsorption dye on the catalyst.

The quantity of catalyst plays an important role in the degradation as well as the commercialization. A low quantity (10 mg/L) of AuAg@C- RGO-CNT-PDA hybrid catalyst exhibits comparatively low degradation compared to a high quantity (200 mg/L). Furthermore, a 10% degradation ability difference was observed in low quantities for the CNT/RGO@PDA-AuAg hybrid catalyst, whereas almost the same amount of degradation was observed in higher quantities. It indicates the AuAg@C-RGO-CNT-PDA hybrid catalyst provides a better platform.

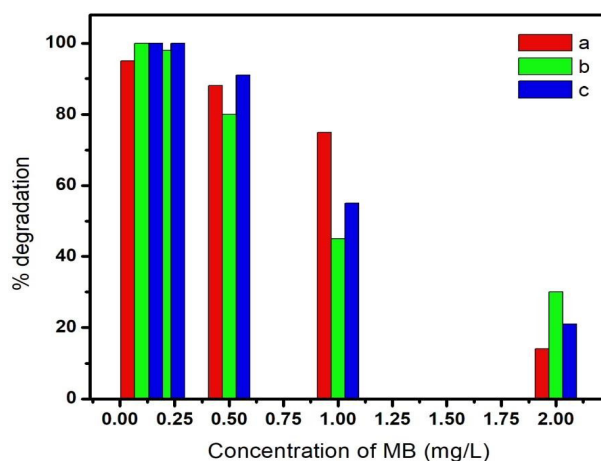


Fig. 8. Catalytic degradation profile of MB with (a) AuAg@C, (b) AuAg@C-Graphene/CNT, (c) AuAg@C-RGO-CNT-PDA hybrid catalyst with H<sub>2</sub>O<sub>2</sub>.

The catalyst exhibits good catalytic activity when reused, and between one and five runs, the catalytic activity drops by 40% while maintaining good stability (Figure 10). This could be due to the adsorption of degraded by-products on the catalyst surface, reducing its efficiency. The catalyst showed low performance for the catalytic reduction of 4-nitrophenol due to the denaturation of the catalyst by borohydride. Hence, we are working to stabilize the composite with polymeric platform to enhance the activity. So we have proceed the catalytic degradation of methylene blue dye.

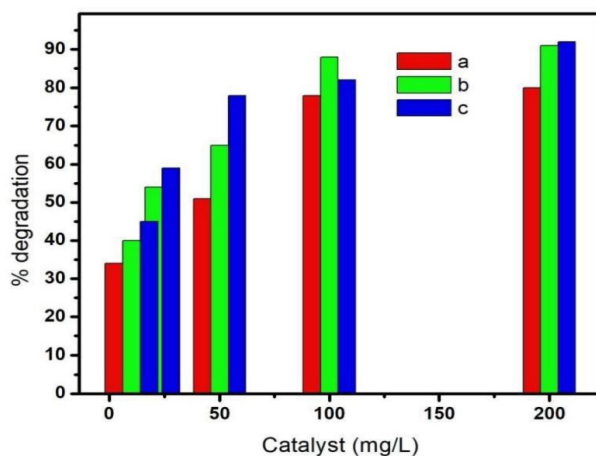


Fig. 9. Effect of catalyst quantity on the MB degradation (a)  $AuAg@C$ , (b)  $AuAg@C$ -Graphene/CNT, (c)  $AuAg@C$ -RGO- CNT-PDA hybrid catalyst with  $H_2O_2$ .

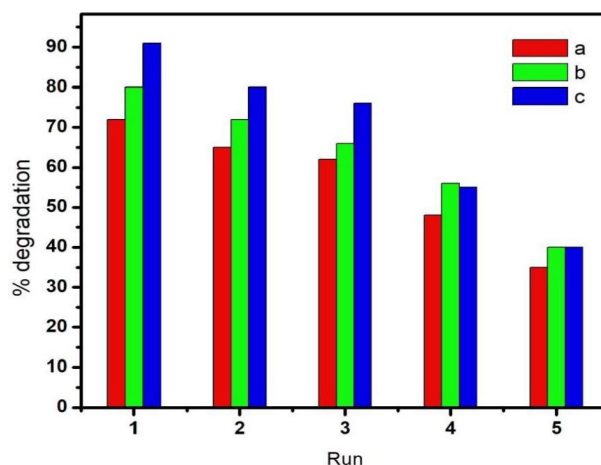


Fig. 10. Effect of reusability on the MB degradation (a)  $AuAg@C$ , (b)  $AuAg@C$ -Graphene/CNT, (c)  $AuAg@C$ -RGO- CNT-PDA hybrid catalyst with  $H_2O_2$ .

#### 4.6. Effect of NaCl concentration on dyedegradation

The commercial effluents and their degradation were performed using mimicked artificial effluents and NaCl solution. The impact of NaCl concentration on the MB dye degradation under ambient conditions is depicted in Figure 11.

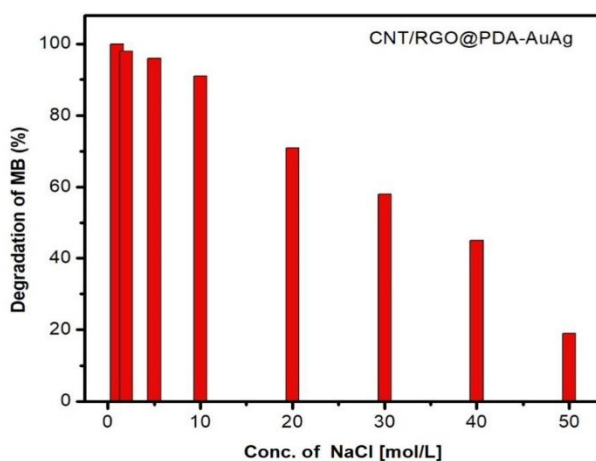


Fig. 11. Effect of NaCl concentration on the degradation of dye.

The experimental results showed that at low concentrations of NaCl solutions, i.e. 5 mol/L, no significant change in MB degradation was observed. However, after 5 mol/L of NaCl was added to the solution mixture, the degradation efficiency was significantly reduced. About 19% degradation was observed in a 50 mol/L NaCl solution.

### Acknowledgements

Authors thank the respective Head of the Institutions for the facilities provided to carry out the research work.

### References

- [1] J. M. Campelo, D. Luna, R. Luque, J. M. Marinas, A.A. Romero, *Chemistry & Sustainability Energy & Materials*, 2(1), 18(2009); <https://doi.org/10.1002/cssc.200800227>
- [2] A. Dhakshinamoorthy, H. Garcia, *Chemical Society Reviews*, 41(15), 5262(2012); <https://doi.org/10.1039/c2cs35047e>
- [3] S. Kalaiarasan, C. Shanthi, *Journal of Ovonic Research*, 18(2), 219(2022); <https://doi.org/10.15251/JOR.2022.182.219>
- [4] N. Narayan, A. Meiyazhagan, R. Vajtai, *Materials*, 12(21), 3602(2019); <https://doi.org/10.3390/ma12213602>
- [5] P. Khandel, R. K. Yadaw, D. K. Soni, L. Kanwar, S. K. Shahi, *Journal of Nanostructure in Chemistry*, 8, 217(2018); <https://doi.org/10.1007/s40097-018-0267-4>
- [6] Z. Gao, R. Su, R. R. Huang, W. Qi, W. He, *Nanoscale Research Letters*, 9, 404(2014); <https://doi.org/10.1186/1556-276X-9-404>
- [7] M. Balamurugan, S. Saravanan, N. Ohtani, *MRS Online Proceedings Library (OPL)*, 1584, pp.jsapmrs13-1584(2014); <https://doi.org/10.1557/opl.2014.279>
- [8] M. Balamurugan, S. Saravanan, *Journal of The Institution of Engineers (India): Series A* 98(4), 461(2017); <https://doi.org/10.1007/s40030-017-0236-9>
- [9] J. Hernández-Ferrer, A.M. Benito, W. K. Maser, E. García-Bordejé, *Catalysts*, 11(11), 1404(2021); <https://doi.org/10.3390/catal11111404>
- [10] D.A. Leal, R. A. Piñales, A. M. P. Rodríguez, B. E. Q. Hidalgo, *Molecules* 26(13), 3813 (2021); <https://doi.org/10.3390/molecules26133813>
- [11] D. A. Yaseen, M. Scholz, *International Journal of Environmental Science and Technology*, 16(2), 1193(2019); <https://doi.org/10.1007/s13762-018-2130-z>
- [12] T. Shindhal, P. Rakholiya, S. Varjani, A. Pandey, H. H. Ngo, W. Guo, H. Y. Ng, M. J. Taherzadeh, *Bioengineered*, 12(1), 70(2020); <https://doi.org/10.1080/21655979.2020.1863034>
- [13] Q. Liu, *IOP Conference Series: Earth and Environmental Science*, 514(5), 052001(2020); <https://doi.org/10.1088/1755-1315/514/5/052001>
- [14] K. J. Vanitha, Kannedo, S. Y. Lau, *Journal of Environmental Chemical Engineering*, 6(4), 4676(2018); <https://doi.org/10.1016/j.jece.2018.06.060>
- [15] K. Sasaki, H. Naohara, Y. Choi, Y. Cai, W. F. Chen, P. Liu, R. R. Adzic, *Nature Communications*, 3(1), 1(2012); <https://doi.org/10.1038/ncomms2124>
- [16] W. S. Hummer, R. E. Offeman, *Journal of the American chemical society*, 80(6), 1339 (1958); <https://doi.org/10.1021/ja01539a017>
- [17] R. Kannan, A. R. Kim, K. S. Nahm, H. K. Lee, D. J. Yoo, *Chemical Communications*, 50(93), 14623(2014); <https://doi.org/10.1039/C4CC06879C>
- [18] P. Kavitha, C. Shanthi, R. Kannan, *Kuwait Journal of Science*, 49(2) 2022; <https://doi.org/10.48129/kjs.12649>
- [19] P. Kavitha, C. Shanthi, R. Kannan, *Digest Journal of Nanomaterials & Biostructures (DJNB)*, 18(1) 2023; <https://doi.org/10.15251/DJNB.2023.181.21>

- [20] R. Kannan, A. R. Kim, K. S. Nahm, D. J. Yoo, Korean Energy Society, 121(2014).
- [21] R. Kannan, H. R. Jang, E. S. Yoo, H. K Lee, D. J. Yoo, RSC Advances, 5(45), pp.35993(2015); <https://doi.org/10.1039/C5RA04226G>
- [22] R. Kannan, A. R. Kim, K. S. Nahm, D. J. Yoo, Journal of Nanoscience and Nanotechnology, 16(3), 2587(2016); <https://doi.org/10.1166/jnn.2016.10769>
- [23] F. Vitale, I. Fratoddi, C. Battocchio, E. Piscopiello, L. Tapfer, M. V. Russo, G. Polzonetti, C. Giannini, Nanoscale Research Letters, 6:102-110(2011); <https://doi.org/10.1186/1556-276X-6-103>
- [24] W. Ding, Y. Liu, Y. Li, Q. Shai, H. Li, H. Xia, D. Wang, X. Tao , RSC Advances, 4:22651(2014); <https://doi.org/10.1039/C4RA03363A>